

# On the Influence of Carbide Formation Upon the Growth Kinetics of Proeutectoid Ferrite in Fe-C-X Alloys

G. J. SHIFLET, H. I. AARONSON, AND J. R. BRADLEY

In the preceding paper, the growth kinetics of grain boundary ferrite allotriomorphs in Fe-C-Si, Fe-C-Mn, Fe-C-Ni, and Fe-C-Cr alloys are reported to be best described by the paraequilibrium model. Significant differences are still observed, however, between the experimentally measured kinetics and those calculated from this model. A TEM study was conducted on these alloys to ascertain whether any of these differences could be attributed to carbide precipitation. In the Fe-C-Mn and Fe-C-Cr alloys, where the measured growth kinetics are low, carbides precipitate on dislocations within the ferrite and are effectively absent, respectively; hence carbide precipitation cannot be responsible for the deviations in these alloys. In the low Ni, Fe-C-Ni alloy, where calculated and measured kinetics agree, carbide precipitation was again found on dislocations in the ferrite. Faster than calculated growth kinetics in the Fe-C-Si and the high Ni, Fe-C-Ni alloys, on the other hand, are attributed in part to carbide precipitation at austenite:ferrite boundaries.

IN an accompanying paper, Bradley and Aaronson<sup>1</sup> (BA) report measurements of the thickening and lengthening kinetics of grain boundary ferrite allotriomorphs as a function of isothermal reaction temperature in single Fe-C-Si, Fe-C-Mn, and Fe-C-Cr alloys and in two Fe-C-Ni alloys. The ability of three models: a) local equilibrium with bulk partition of alloying element,<sup>2-10</sup> b) local equilibrium with localized pileup but no bulk partition of alloying element,<sup>10-14</sup> and c) paraequilibrium,<sup>14-18</sup> to account for these data is quantitatively examined. Although it is concluded that the paraequilibrium model best explains the data, significant discrepancies remain between calculated and measured growth kinetics even for this model. While good agreement is obtained for the low Ni, Fe-C-Ni alloy, growth faster than calculated is found for the Fe-C-Si and the high Ni, Fe-C-Ni alloys and slower than calculated for the Fe-C-Mn and Fe-C-Cr alloys. Although several explanations are considered by BA, an obvious one, clearly in need of experimental testing, is that of carbide precipitation at austenite:ferrite boundaries. This can occur either as interphase boundary carbide precipitation on planar or on (apparently) curved austenite:ferrite boundaries, or as pearlite-like fibrous carbide precipitation.<sup>19-20</sup> Such precipitation might slow down

the growth of ferrite by pinning the austenite:ferrite boundaries.<sup>21</sup> Alternatively, these carbides could increase the growth kinetics of mobile areas of the austenite:ferrite boundaries by steepening the carbon concentration gradient in austenite driving their growth. Accordingly, the present investigation was undertaken to study this question in the BA alloys within the temperature-time envelopes employed for the growth kinetics studies. The observations reported here also supplement the literature on carbide precipitation per se in Fe-C-X alloys. With the exception of Cr, the alloying elements used are not strong carbide-formers and their effects upon the formation of carbides in association with proeutectoid ferrite have not been as intensively studied.

## EXPERIMENTAL PROCEDURE

The composition of the alloys used in this investigation are given in Table I of BA.<sup>1</sup> The same heat treatment procedure was utilized. Somewhat larger specimens,  $0.013 \times 0.013 \times 0.00025$  m, were employed to facilitate transmission electron microscopy (TEM) studies. These specimens were chemically thinned to ca.  $7 \times 10^{-5}$  m using a solution described by Plichta *et al*.<sup>22</sup> Discs  $3 \times 10^{-3}$  m in diameter punched from the specimens were thinned to perforation with a Fischione twin jet electropolisher using an electrolyte consisting of  $2.5 \times 10^{-4}$  m<sup>3</sup> glacial acetic acid,  $7.5 \times 10^{-2}$  kg anhydrous sodium chromate,  $2.5 \times 10^{-2}$  kg chromic oxide and  $10^{-5}$  m<sup>3</sup> water at room temperature under a potential of ca. 60 volts. The thinned discs were examined with Philips EM301G and JEOL 100CX electron microscopes. Ferrite containing areas were examined in each specimen until the various types of observation had been repeated with sufficient frequency to assure the investigators that a representative proportion of the specimen had been examined.

G. J. SHIFLET, formerly Republic Steel Fellow, Department of Metallurgical Engineering, Michigan Technological University, Houghton, MI 49931 and Visiting Graduate Student, Carnegie-Mellon University, Pittsburgh, PA 15213, is now Assistant Professor, University of Virginia, Department of Materials Science, Charlottesville, VA 22901. H. I. AARONSON, formerly Professor, Department of Metallurgical Engineering, Michigan Technological University, is now R. F. Mehl Professor, Department of Metallurgical Engineering and Materials Science, Carnegie-Mellon University, Pittsburgh, PA 15213. J. R. BRADLEY, formerly Graduate Student, Department of Metallurgical Engineering, Michigan Technological University, is now with the Physics Department, General Motors Research Laboratories, Warren, MI 48090.

Manuscript submitted February 23, 1981.

## RESULTS

*Fe-0.13 Pct C-2.99 Pct Cr.* Previous TEM studies of carbide formation in Fe-C-Cr alloys have been mainly in alloys whose chromium content exceeds the 3 pct used in this study.<sup>23-27</sup> A variety of carbide morphologies was found in association with ferrite including interphase boundary carbides, fibrous carbides and also idiomorphs at ferrite:ferrite grain boundaries. The type of carbide formed was dependent upon composition;  $M_{23}C_6$ ,  $M_7C_3$ , and  $M_3C$  were identified.

The TTT-curve for the initiation of the proeutectoid ferrite reaction in this alloy, reproduced in Fig. 1(a) from the work of Aaronson and Domian,<sup>29</sup> exhibits a bay, the deepest portion of which is at ca. 600 °C. Specimens were isothermally reacted at 700, 650, and 600 °C. Optical microscopy revealed (Fig. 2(a)) that ferrite grows along austenite grain boundaries at all three temperatures. The ferrite is blocky in appearance at 700 °C but becomes more ragged at lower temperatures. TEM studies showed that, within the reaction time ranges employed by BA, all ferrite examined appeared to be free of carbides (Fig. 3). Some exceedingly fine precipitates *may* have been present on dislocations, though this observation could not be confirmed. However, it is quite certain that neither interphase boundary nor fibrous carbides appeared in any of the ferrite observed.

*Fe-0.12 Pct C-3.08 Pct Mn.* No previous TEM studies of carbide precipitation in association with ferrite appear to have been reported in Fe-C-Mn alloys. The TTT-curve for the beginning of austenite decomposition in this alloy is given in Fig. 1(b).<sup>29</sup> Optical microscopy showed that proeutectoid ferrite morphology evolved progressively from predominantly grain boundary allotriomorphs at 650 °C to blockier allotriomorphs with some secondary sawteeth at 600 °C (Fig. 2(b)), and secondary sideplates at almost all grain boundaries at 550 °C. TEM revealed carbides only at 600 °C (Fig. 4(a)). Imaging the carbides in dark field clearly showed them to lie on dislocations (Fig. 4(b)). At 650 and 550 °C, no carbides were seen in any of the ferrite examined.

*Fe-0.11 Pct C-3.28 Pct Ni.* Chilton and Speich<sup>30</sup> observed cementite precipitation on dislocations within the ferrite as well as interphase boundary precipitation of carbides in several Fe-C-Ni alloys. The TTT-curve for the alloy used in this study is given in Fig. 1(c).<sup>29</sup> Optical microscopy showed a blocky allotriomorphic microstructure with secondary sawteeth at 715 °C (Fig. 2(c)); secondary sideplates began to develop at 650 °C. At 715 °C, TEM showed carbide precipitation as an allotriomorph-like morphology nucleated on dislocations (Fig. 5). Dark-field observations demonstrated that the carbides in a given ferrite grain can take up at least three different orientations when precipitated on dislocations (Figs. 5(b) through (d)). At 650 °C, ferrite free of carbide precipitation was observed as well as precipitation on dislocations.

*Fe-0.40 Pct C-1.73 Pct Si.* No prior TEM investigations of carbide precipitation in hypoeutectoid Fe-C-Si alloys have been located. The TTT-curve for this alloy is given in Fig. 1(d).<sup>29</sup> Microstructures at two

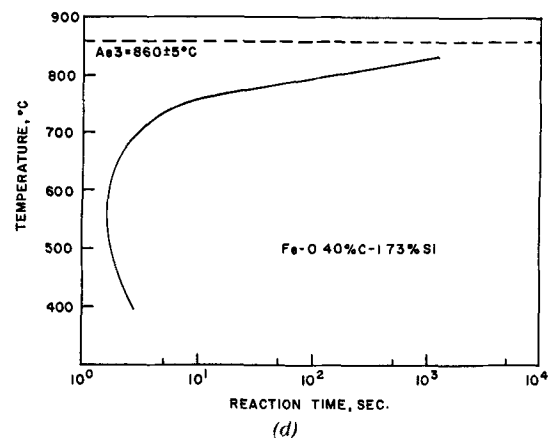
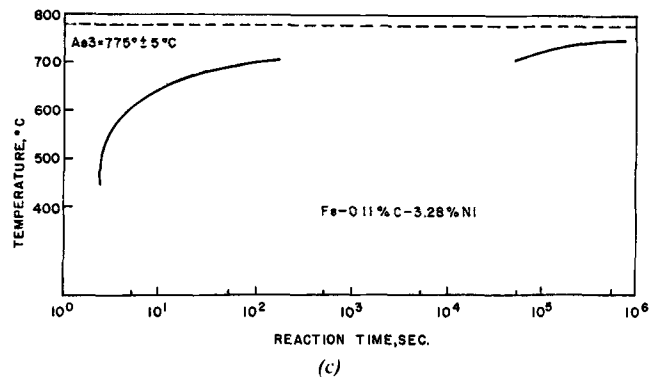
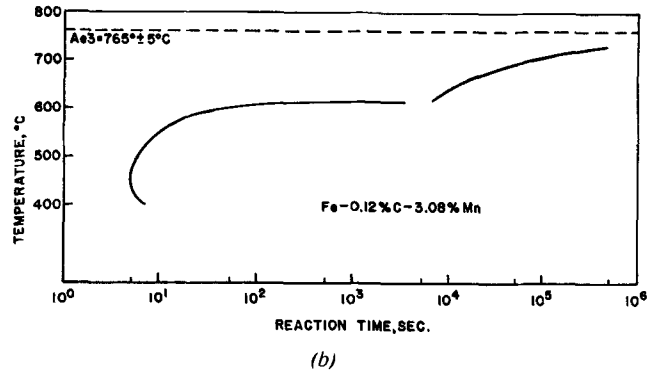
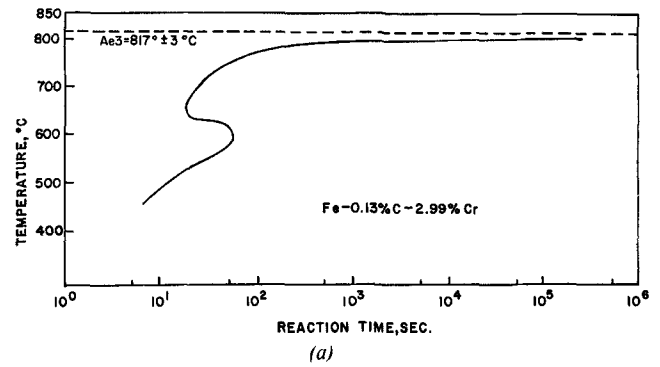


Fig. 1—TTT-diagrams for initiation of transformation in: (a) Fe-0.13 pct C-2.99 pct Cr, (b) Fe-0.12 pct C-3.08 pct Mn, (c) Fe-0.11 pct C-3.28 pct Ni, and (d) Fe-0.40 pct C-1.73 pct Si.<sup>29</sup>

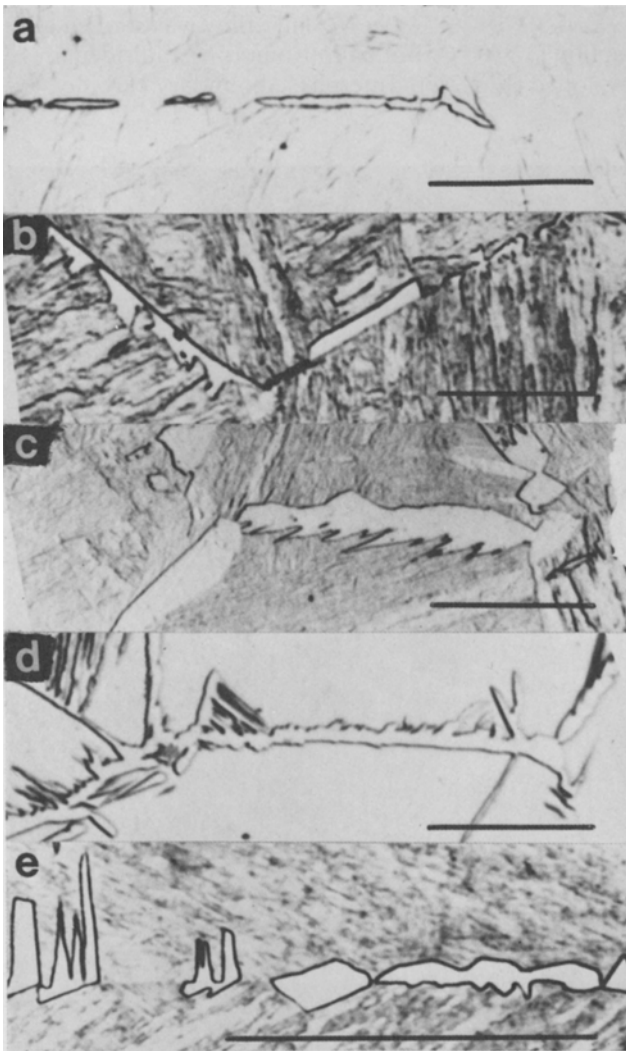


Fig. 2—(a) Fe-0.13 pct C-2.99 pct Cr, reacted 10 s at 700 °C, growth of ferrite along austenite grain boundaries; (b) Fe-0.12 pct C-3.08 pct Mn, reacted 360 s at 600 °C, grain boundary ferrite allotriomorphs and secondary sawteeth; (c) Fe-0.11 pct C-3.28 pct Ni, reacted 120 s at 715 °C, illustrating the development of ferrite allotriomorphs and secondary sawteeth; (d) Fe-0.40 pct C-1.73 pct Si, reacted 5 s at 700 °C, a typical illustration of grain boundary ferrite allotriomorphs with many sideplates developed from them; (e) Fe-0.43 pct C-7.51 pct Ni, reacted 300 s at 550 °C, grain boundary ferrite allotriomorphs and sideplates. The marker in each micrograph represents 47  $\mu\text{m}$ .

temperatures, 700 and 750 °C, were studied. Figure 2(d) shows ferrite allotriomorphs with many secondary sideplates, a typical optical microstructure at these temperatures. A low magnification TEM micrograph (Fig. 6(a)) displays a similar microstructure. A higher magnification view of area “B” in Fig. 6(a), located within a secondary sideplate, demonstrates that the ferrite is relatively free of carbide precipitation (Fig. 6(b)), whereas area “A”, located in the blocky allotriomorph from which the sideplate developed and shown by SAD to be part of the same ferrite grain, exhibits copious precipitation on dislocations (Fig. 6(c)). A sawtooth in a different ferrite grain also shows precipitation on dislocations (Fig. 7).

Interphase boundary precipitation of carbides was seen at 700 °C. This type of precipitation did not occur as often as that on dislocations. The characteristic rows

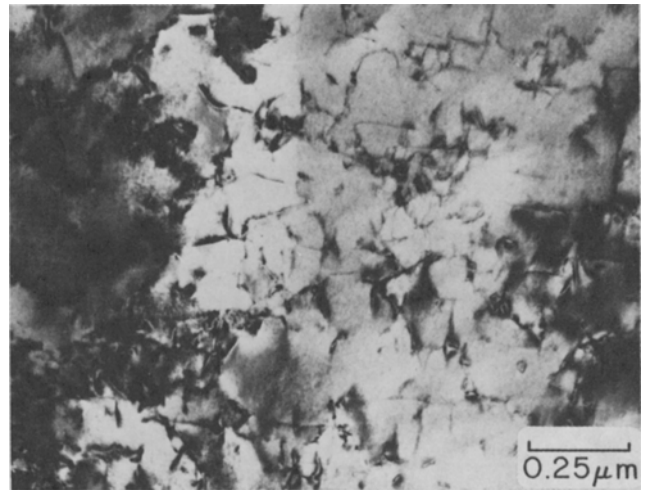


Fig. 3—Fe-0.13 pct C-2.99 pct Cr, reacted 20 s at 650 °C, illustrating absence of carbides within ferrite.

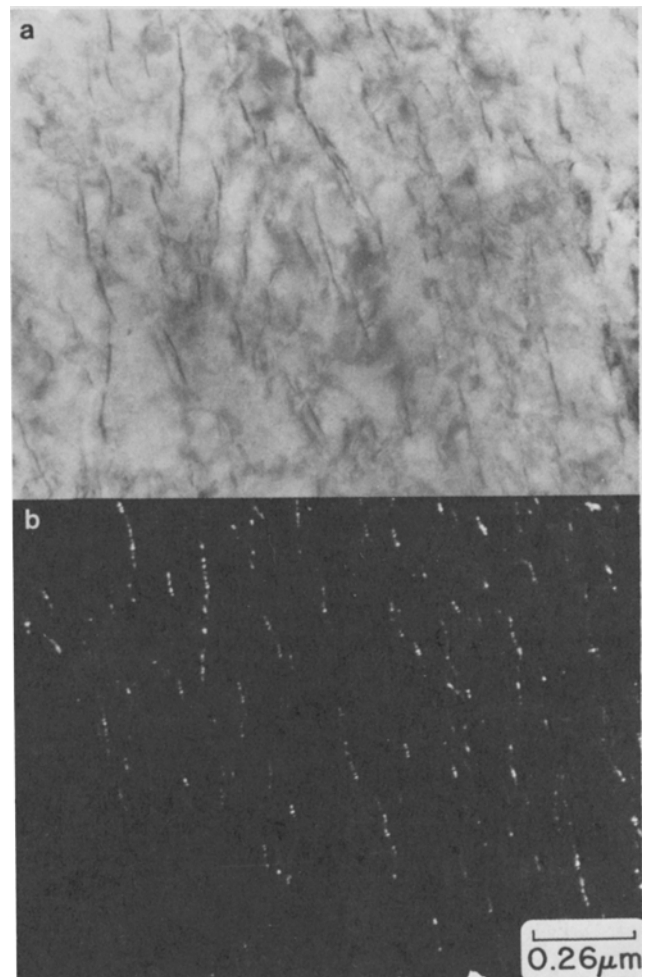


Fig. 4—Fe-0.12 pct C-3.08 pct Mn, reacted 360 s at 600 °C: (a) bright field view of carbides within ferrite; (b) dark field view of the same area showing that the carbides lie along dislocations.

of carbides are displayed through use of a diffracted beam from the carbides in Fig. 8. Ledges are present at the arrowed ferrite:austenite (now martensite) boundaries. Carbides are seen to have precipitated at the broad faces of the ledges. Carbide precipitations on

dislocations was also observed at 750 °C, but no interphase boundary carbides were seen at this temperature.

*Fe-0.43 Pct C-7.51 Pct Ni*. This alloy was studied after reaction at 550 °C. Both allotriomorphs and sideplates developed (Fig. 2(e)). Interphase boundary carbide

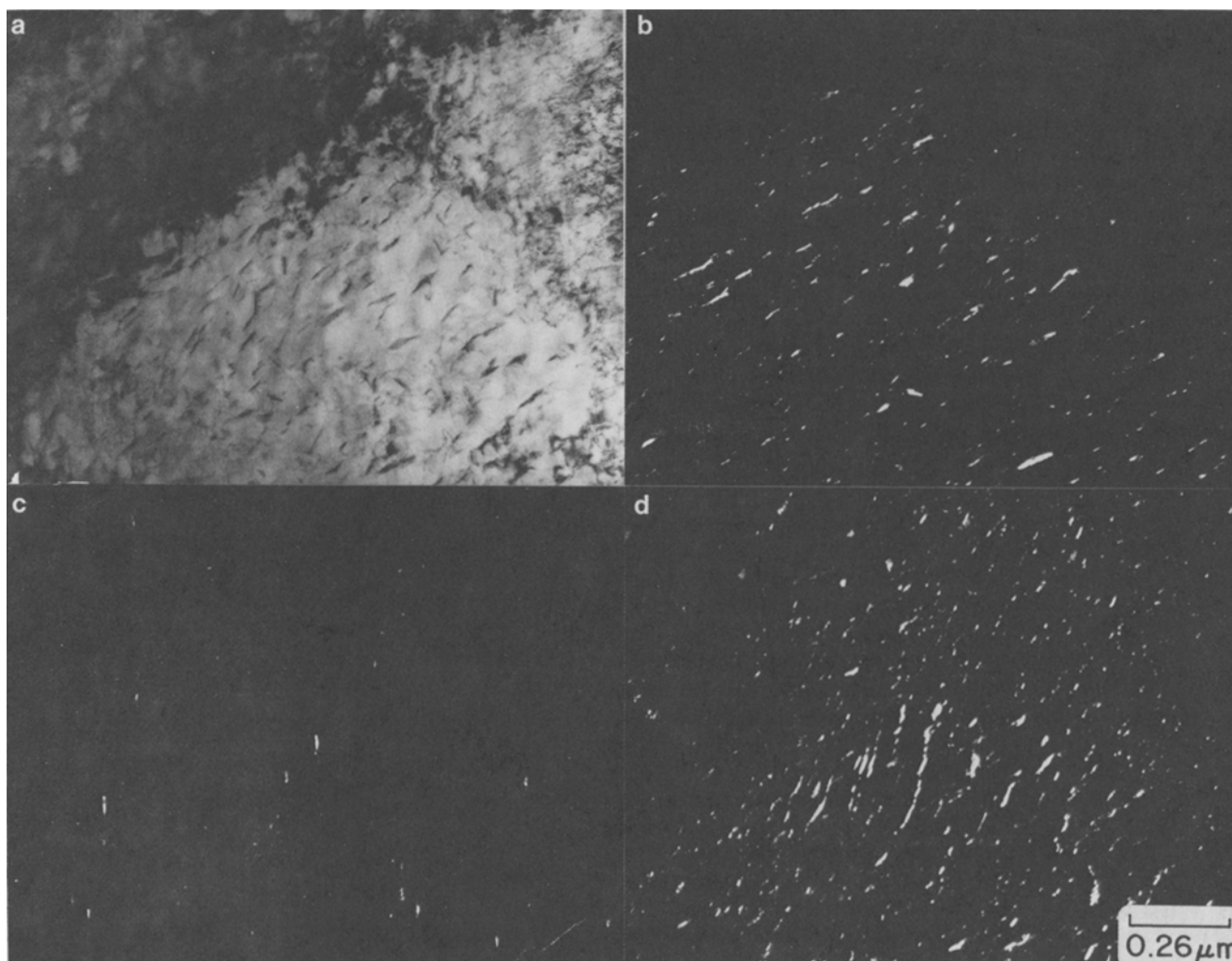


Fig. 5—Fe-0.11 pct C-3.28 pct Ni, reacted 120 s at 715 °C, showing a portion of the area in Fig. 2(c): (a) in bright field, and (b), (c) and (d) in dark field, imaged in three different carbide reflections.

**Table I. Summary of TEM Observations and Growth Kinetics<sup>1</sup> Data**

Alloy	Reaction Temperature, °C	Longest Isothermal Reaction Time Studied, s <sup>1</sup>	Carbide Precipitation	$\alpha_{\text{corr}}/\alpha_{\text{para}}^1$
Fe-0.13 pct C-2.99 pct Cr	700	15	None	00.52
	650	5	None	00.20
	600	5	None	00.17
Fe-0.12 pct C-3.08 pct Mn	650	4800	None	00.04
	600	360	On Dislocations	00.22
	550	16	None	00.41
Fe-0.11 pct C-3.28 pct Ni	715	120	On Dislocations	00.67
	650	8	On Dislocations	00.82
Fe-0.40 pct C-1.73 pct Si	800	144	On Dislocations	12.27
	750	25	On Dislocations	2.54
	700	5	On Dislocations & IBP (rare)	2.13
Fe-0.43 pct C-7.51 pct Ni	550	300	IBP (rare)	1.61

IBP = interphase boundary precipitation

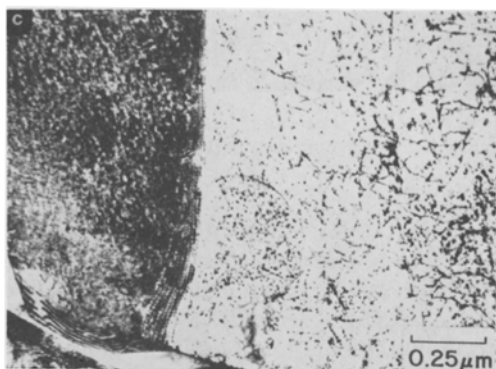
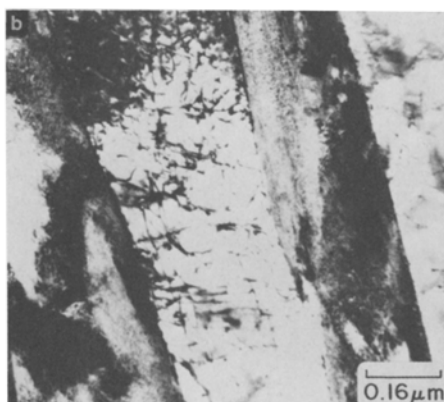
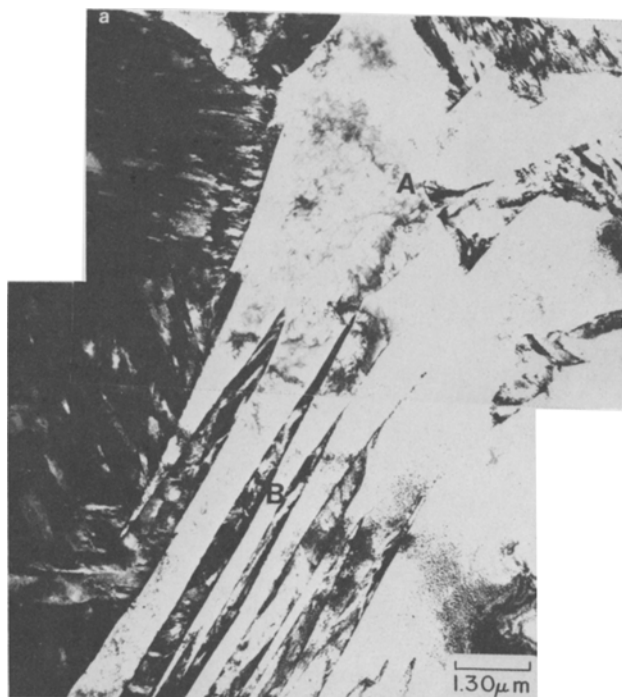


Fig. 6—Fe-0.40 pct C-1.73 pct Si, reacted 5 s at 700 °C: (a) a microstructure similar to that of Fig. 2(d); (b) higher magnification view of area marked “B” in (a), showing near absence of carbide precipitation within a secondary sideplate; (c) higher magnification view of area marked “A” in (a), illustrating extensive carbide precipitation within a blocky ferrite allotriomorph.

precipitation was identified in association with a small fraction of the ferrite crystals examined (Fig. 9). The discrete nature of the carbides demonstrates that this is not a fibrous structure. Dark field experiments revealed no other orientations of carbides present, proving that the carbides did not precipitate on dislocations within the ferrite grains. In many ferrite grains, carbide precipitation was absent.

#### Crystal Structure of the Carbides

Due to the small size of the carbides, identification of their crystal structure was often difficult. However, all SAD patterns obtained could be indexed in accordance with the complex orthorhombic structure of  $M_3C$  (Fig. 10), *i.e.*,  $(Fe,X)_3C$  or cementite. In the Fe-C-Si alloy, the concentration of Si in the carbide was presumably very small.<sup>31</sup> This result is consistent with the earlier work of Lyman and Troiano,<sup>32</sup> Chilton and Speich<sup>30</sup> and Hultgren.<sup>33,34</sup> They studied a wide range of F-C-X alloys, including compositions approximating those used in this study. In all alloys containing less than 5 pct X, the initial carbide in the nonpearlitic transformation products was  $M_3C$ .

#### DISCUSSION

The influence, if any, of carbide precipitation on the growth kinetics of ferrite depends on where such precipitation occurs. In the Mn and the 3.28 pct Ni alloys, when carbide precipitation was observed it appeared only on dislocations. BA found that the experimentally determined growth kinetics are slower than those predicted from the paraequilibrium model in the Mn alloy and about equal in the 3.28 pct Ni alloy. Further, the only carbide precipitation observed in the Si alloy at 750 and 800 °C appeared on dislocations, where the measured growth kinetics were more rapid than those calculated. This absence of any correlation between growth kinetics and carbide precipitation on dislocations is consistent with the expectation that carbide precipitation behind advancing austenite:ferrite boundaries should have negligible influence upon the interface compositions and thus upon the growth kinetics of these boundaries.

The absence of detectable carbide precipitation within the BA reaction temperature-time “envelope” in the Cr alloy demonstrates that the slower than calculated growth kinetics of ferrite in this alloy also cannot be explained through pinning of austenite:ferrite boundaries by carbides. Boswell *et al*<sup>35</sup> have shown that the TTT-curve for the initiation of transformation in an Fe-0.11 pct C-1.95 pct Mo alloy is nearly the mirror image of the  $\alpha$  vs temperature plot, where  $\alpha$  is the parabolic rate constant for thickening of grain boundary allotriomorphs. Although degeneracy of the ferrite morphologies prevented the measurement of  $\alpha$  at temperatures below that of the bay in the Cr alloy, an essentially similar situation evidently obtains in this alloy.

Interphase boundary carbides were occasionally observed at the one reaction temperature studied in the 7.51 pct Ni alloy and also at the lowest temperature

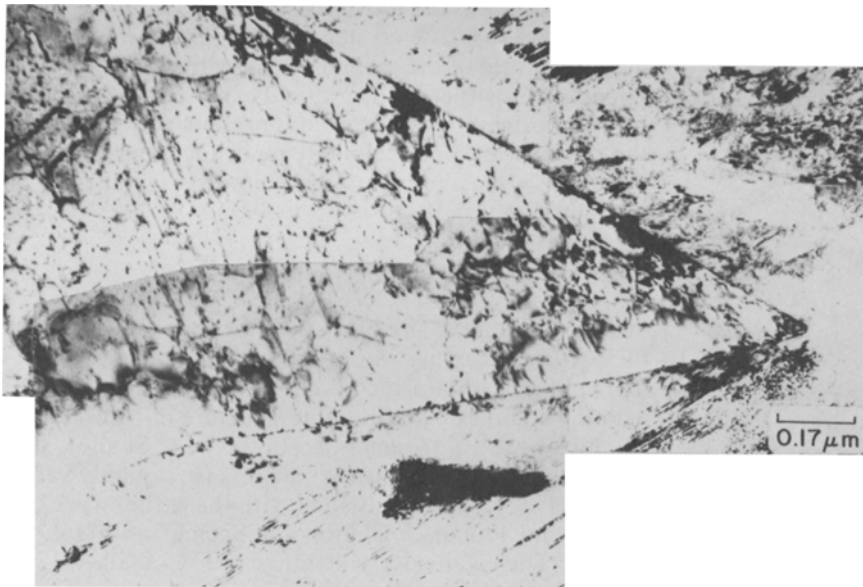


Fig. 7—Fe-0.40 pct C-1.73 pct Si, reacted 5 s at 700 °C, showing precipitation on dislocations in a ferrite sawtooth.

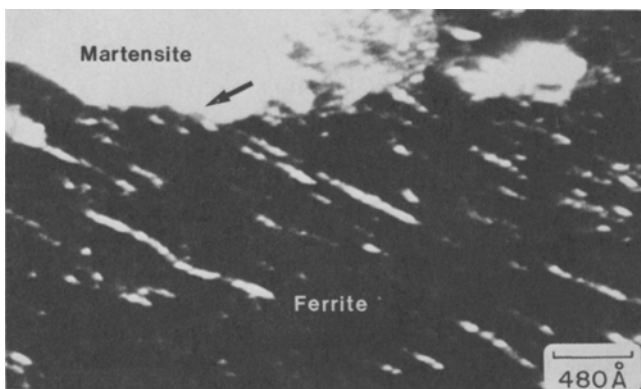


Fig. 8—Fe-0.40 pct C-1.73 pct Si, reacted 5 s at 700 °C; interphase boundary carbides shown in dark field.

utilized in the Si alloy. At both temperatures  $\alpha$  is about twice that calculated from the paraequilibrium model. The acceleration of growth thus observed can be explained in terms of the influence of carbides upon both the ledge mechanism and the “bowing around” mechanism<sup>20</sup> for the thickening of ferrite allotriomorphs in the presence of interphase boundary carbides. The spacing between ledges can be decreased. Additionally, since these carbides are in contact with austenite, they increase the driving force for the migration of the mobile areas of the austenite:ferrite boundaries from the difference between the carbon contents corresponding to the extrapolated Ae<sub>3</sub> and the bulk composition of the alloy to the difference between the carbon contents represented by the extrapolated Ae<sub>3</sub> and the extrapolation of the relevant (austenite)/(austenite + carbide) phase boundary, both at the reaction temperature used. However, the circumstance that no interphase boundary carbides were observed in the Si alloy at 750 and 800 °C indicates that this explanation is incomplete.

Following an earlier proposal,<sup>36</sup> BA suggested that the higher  $\alpha$  values might result from an “inverse solute drag-like effect” induced by the segregation of Si, and

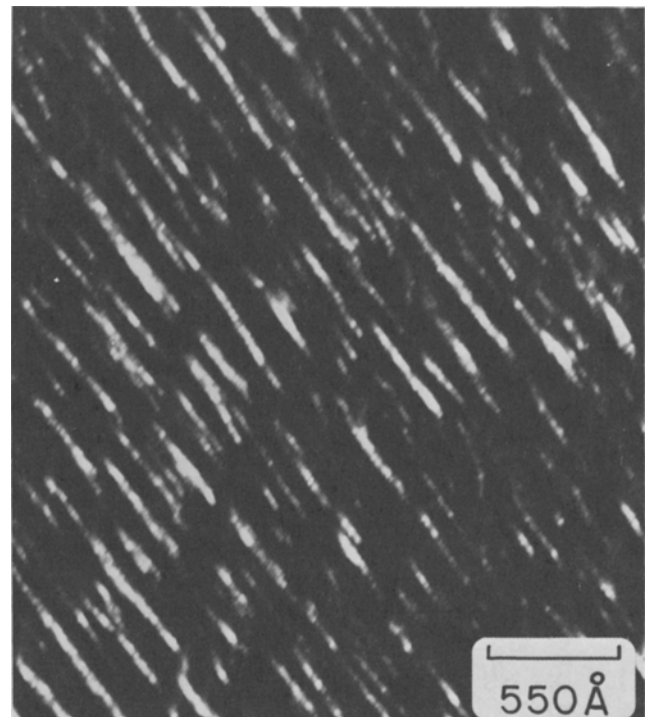


Fig. 9—Fe-0.43 pct C-7.51 pct Ni, reacted 300 s at 550 °C: dark field micrograph of interphase boundary carbide precipitation.

to a lesser extent of Ni, to disordered (and thus mobile) austenite:ferrite boundaries. Since Si markedly increases the activity of carbon in austenite,<sup>37</sup> as does Ni, less effectively,<sup>37</sup> such segregation would raise the concentration gradient of carbon in austenite driving the growth of ferrite and thus  $\alpha$ . Both the interphase boundary carbide and the inverse solute drag-like effects may well be operative in the Si and the higher Ni alloys. Interphase carbide precipitation could have escaped detection by TEM at 750 and 800 °C in the Si alloy because of its scarcity. However, since  $\alpha$  is

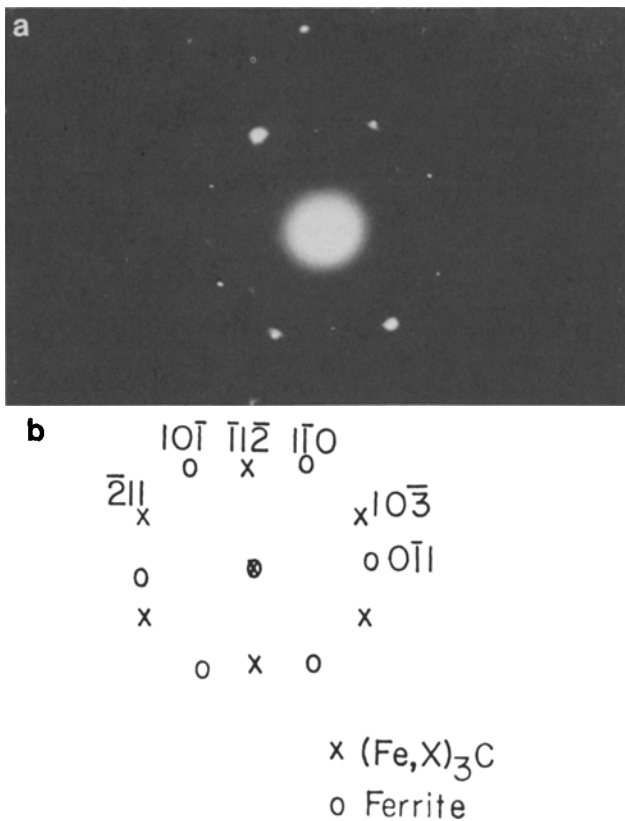


Fig. 10—Fe-0.11 pct C-3.08 pct Mn, reacted 360 s at 600 °C: (a) [351] zone axis of  $(\text{Fe},X)_3\text{C}$  and [111] zone axis of ferrite; (b) indexed schematic of electron diffraction pattern in (a).

determined from a plot of the thickness of the thickest allotriomorph as a function of the square root of the isothermal reaction time, this form of carbide precipitation would have affected the measured growth kinetics even if it took place very infrequently. The possible role of interphase boundary carbides in accelerating the growth of ferrite allotriomorphs in the Si and Ni alloys is urged here because Abe *et al.*<sup>38</sup> have secured clear evidence that such carbides do increase  $\alpha$  in an Fe-C-V alloy, where this form of carbide precipitation is ubiquitous.<sup>39</sup>

### SUMMARY

The Fe-C-X alloys (where X is Si, Mn, Ni, or Cr) used by Bradley and Aaronson (BA)<sup>1</sup> in the preceding paper to determine alloying element effects upon the growth kinetics of grain boundary allotriomorphs of proeutectoid ferrite have been investigated by TEM within the same reaction temperature-reaction time envelopes to evaluate the effects of carbide precipitation upon allotriomorph growth kinetics. BA found that the paraequilibrium model<sup>14-18</sup> for the chemistry of austenite and ferrite in the vicinity of austenite:ferrite boundaries is the most appropriate one, of the three they examined, for allotriomorph growth kinetics in their alloys. They also noted, however, a number of instances in which the ratio of the corrected experimental parabolic rate constant for allotriomorph thickening,  $\alpha_{\text{corr}}$ , to the rate constant calculated from the

paraequilibrium model,  $\alpha_{\text{para}}$ , is significantly different from unity. In this study, the role of carbide precipitation in producing these deviations was experimentally assessed.

Table I summarized the TEM observations on carbide precipitation made during this study and the  $\alpha_{\text{corr}}/\alpha_{\text{para}}$  ratios obtained by BA under the same conditions. Most of the carbide precipitation observed took place on dislocations. As anticipated, there is no correlation between such precipitation and the growth kinetics ratio. In the Cr alloy, where  $\alpha$  behaves in a manner quite different from that predicted, no carbide precipitation could be definitely identified. Interphase boundary carbide precipitation<sup>19</sup> was the only other type of carbide formation discerned. Such precipitation was found at but one temperature in the Si alloy and in the higher Ni alloy.  $\alpha_{\text{corr}}/\alpha_{\text{para}} > 1$  in both of these alloys, and interphase boundary carbide precipitation may well have been responsible for at least part of this deviation. However, as noted by BA, an “inverse solute drag-like” effect<sup>36</sup> due to segregation of either Si or Ni to disordered areas of austenite:ferrite boundaries, may also have been responsible.

### ACKNOWLEDGMENTS

Most of the contributions made by GJS at Michigan Technological University were supported by a Republic Steel Corporation Fellowship, while his work at Carnegie-Mellon University was largely funded by NSF Grant DMR79-17018 from the Division of Materials Research. The balance of his efforts and all those of JRB and HIA were funded by contracts from the Army Research Office with both MTU and CMU, most recently by DAAG29-80-C-0018. CJM central facilities were used during research at CMU. All of this support is gratefully acknowledged.

### REFERENCES

1. J. R. Bradley and H. I. Aaronson: *Metall. Trans. A*, 1981, vol. 12A, p. 1729.
2. G. R. Purdy, D. H. Weichert, and J. S. Kirkaldy: *Trans. TMS-AIME*, 1964, vol. 230, p. 1025.
3. J. B. Gilmour, G. R. Purdy, and J. S. Kirkaldy: *Metall. Trans.*, 1972, vol. 3, p. 3213.
4. R. C. Sharma and J. S. Kirkaldy: *Can. Metall. Q.*, 1973, vol. 12, p. 391.
5. H. Oikawa, J. F. Remy, and A. G. Guy: *Trans. Am. Soc. Met.*, 1968, vol. 61, p. 110.
6. D. J. Swinden and J. H. Woodhead: *J. Iron Steel Inst.*, 1971, vol. 209, p. 583.
7. D. V. Edmonds and R. W. K. Honeycombe: *Met. Sci.*, 1978, vol. 12, p. 399.
8. F. Togashi and T. Nishizawa: *J. Jpn. Inst. Met.*, 1976, vol. 40, p. 12.
9. G. R. Purdy and J. S. Kirkaldy: *Trans. TMS-AIME*, 1963, vol. 227, p. 1255.
10. J. S. Kirkaldy: *Can. J. Phys.*, 1958, vol. 36, p. 907.
11. A. A. Popov and M. S. Mikhalev: *Phys. Met. Metallogr.*, 1959, vol. 7, p. 36.
12. L. S. Darken and R. M. Fisher: *Decomposition of Austenite by Diffusional Processes*, p. 249, Interscience Publishers, New York, NY, 1962.
13. M. Hillert: *The Mechanism of Phase Transformations in Crystalline Solids*, p. 231, Institute of Metals, London, 1969.
14. M. Hillert: Internal Report, Swedish Inst. for Metals Research, Stockholm, Sweden, 1953.

15. A. Hultgren: *Jernkontorets Ann.*, 1951, vol 135, p. 403.
16. M. Hillert: *Jernkontorets Ann.*, 1952, vol. 136, p. 25.
17. E. Rudberg: *Jernkontorets Ann.*, 1952, vol. 136, p. 91.
18. J. B. Gilmour, G. R. Purdy, and J. S. Kirkaldy: *Metall. Trans.*, 1972, vol. 3, p. 1455.
19. R. W. K. Honeycombe: *Metall. Trans. A*., 1976, vol. 7A, p. 915.
20. R. W. K. Honeycombe: *Met. Sci.*, 1980, vol. 14, p. 201.
21. G. R. Purdy: *Acta Metall.*, 1978, vol. 26, p. 487.
22. M. R. Plichta, H. I. Aaronson, and W. F. Lange: *Metallography*, 1976, vol. 9, p. 455.
23. M. Mannerkoski: *Acta Polytech. Scand.*, 1964, chapt. 26.
24. M. Mannerkoski: *Met. Sci. J.*, 1969, vol. 3, p. 54.
25. K. Campbell and R. W. K. Honeycombe: *Met. Sci. J.*, 1974, vol. 8, p. 197.
26. P. R. Howell, R. A. Ricks, J. V. Bee, and R. W. Honeycombe: *Philos. Mag. A*, 1980, vol. 41, no. 2, p. 165.
27. P. R. Howel, J. V. Bee, and R. W. K. Honeycombe: *Metall. Trans. A*, 1979, vol. 10A, p. 1213.
28. J. V. Bee, P. R. Howell, and R. W. K. Honeycombe: *Metall. Trans. A*, 1979, vol. 10A, p. 1207.
29. H. I. Aaronson and H. A. Domian: *Trans. TMS-AIME*, 1966, vol. 236, p. 781.
30. J. M. Chilton and G. R. Speich: *Metall. Trans.*, 1970, vol. 1, p. 1019.
31. W. S. Owen: *J. Iron Steel Inst.*, 1951, vol. 167, p. 117.
32. T. Lyman and A. R. Troiano: *Trans. Am. Soc. Met.*, 1946, vol. 37, p. 402.
33. A. Hultgren: *Trans. Am. Soc. Met.*, 1947, vol. 39, p. 915.
34. A. Hultgren: *K. V. A. Handl.*, 1953, vol. 4, no. 3.
35. P. G. Boswell, K. R. Kinsman, and H. I. Aaronson: unpublished research, Ford Motor Co., Dearborn, MI, 1968.
36. K. R. Kinsman and H. I. Aaronson: *Metall. Trans.*, 1973, vol. 4, p. 959.
37. J. S. Kirkaldy, B. A. Thomson, and E. A. Baganis: *Hardenability Concepts with Applications to Steel*, p. 82, TMS-AIME, Warrendale, PA, 1978.
38. T. Abe, H. I. Aaronson, and G. J. Shiflet: unpublished research, Carnegie-Mellon University, Pittsburgh, PA, 1980.
39. A. D. Batte and R. W. K. Honeycombe: *J. Iron Steel Inst.*, 1973, vol. 211, p. 284.